THE ASTROPHYSICAL JOURNAL, 238:45–53, 1980 May 15

AN EXTENDED NEBULOSITY OF HIGHLY IONIZED GAS IN THE SB0 SEYFERT GALAXY NGC 3516: DETECTION AND STUDY OF THE PHYSICAL CONDITIONS OF THE GAS

MARIE-HELENE ULRICH[1,2]
European Southern Observatory, Geneva
AND
D. PÉQUIGNOT
Observatoire de Meudon
Received 1979 August 13; accepted 1979 November 7

ABSTRACT

We present spectrographic and spectrophotometric observations of a nebulosity of ionized gas surrounding the nucleus of the Seyfert galaxy NGC 3516. The nebulosity consists of an extended region of weak emission which is detected up to 7 kpc from the nucleus and in which are embedded bright clouds or filaments. The intensities of 14 emission lines, including [O III] λ4363 and He II λ4686, have been measured in one of the brightest gas clouds located at 2 kpc from the center.

We have calculated photoionization models for this bright cloud in which the ionizing source is the central nonthermal source. Charge-transfer reactions of several ions with H^0 and, in particular, a charge-transfer rate coefficient for O^{++} of 8×10^{-10} cm^3 s^{-1} are included in the models. Good agreement with the observations is obtained, using a model where the cloud is nearly optically thick and has a uniform density $n_H \approx 30$ cm^{-3}, i.e., a density definitely smaller than the density $n_e \approx 1000$ cm^{-3} in the narrow-line region in the nucleus. The abundances of the extranuclear gas are nearly normal. The total mass of the nebulosity is at least $10^7\ M_\odot$.

The photoionization models are valid for any nebulosity illuminated by a power-law spectrum and where the collisional de-excitation can be neglected ($n_H < 10^3$ cm^{-3}).

The data are consistent with the following possible origins for the extended gaseous nebulosity: the gas has been expelled by the Seyfert nucleus and now forms a large, low-density nebulosity or, alternatively, the ionized gas which we have detected at large distances from the nucleus could be ambient gas which would have remained undetected optically if the galaxy did not have a Seyfert nucleus with an intense ionizing source.

Subject headings: galaxies: individual — galaxies: internal motions — galaxies: nuclei — galaxies: Seyfert — galaxies: structure

I. INTRODUCTION

NGC 3516 is an exceptionally interesting nearby Seyfert galaxy. First, NGC 3516 has a very active nucleus, where both the continuum radiation and the permitted lines vary in intensity (de Vaucouleurs and de Vaucouleurs 1972; Andrillat and Souffrin 1973). Second, NGGC 3516 is of morphological type SB0, whereas the majority of the Seyfert galaxies are of types Sa to Sc. It therefore provides an opportunity to investigate the extended emission which could be present outside the nucleus, without interference by the emission from the normal H II regions of spiral galaxies.

In this article, we present spectrographic and spectrophotometric observations of a nebulosity of highly excited gas surrounding the nucleus of NGC 3516. This nebulosity is formed by some bright clouds, embedded in a large region which emits weak lines and extends up to 7 kpc from the nucleus.

We measured the velocity field of the ionized nebulosity from long-slit spectra and measured the intensities of the emission lines in the bright clouds with an Image Dissector Scanner (IDS); these spectrophotometric data form the basis for an analysis of the physical conditions of the gas in the extranuclear region.

The results of the observations are presented in § II. Models for the gas clouds are presented in § III. The possible effects of the central ionizing source on ambient gas which could be present in the disk are discussed in § IV.

II. OBSERVATIONS

a) Spectrographic Observations—Velocity of the Gas

The first indication of the possible presence of an extended nebulosity of ionized gas around the nucleus of NGC 3516 comes from the monochromatic image-tube photographs taken by Adams (1977). We first

[1] Visiting Astronomer, Kitt Peak National Observatory, which is operated by the Association of Universities for Research in Astronomy, Inc., under contract with the National Science Foundation.

[2] Also at the University of Texas at Austin during part of this investigation.

TABLE 1

SUMMARY OF SPECTROSCOPIC OBSERVATIONS[a]

Spectrum Number	Exposure (min)	Position Angle (degrees)	Position of Spectrograph Slit
1328	60	0	4.5″ E of nucleus
1329	75	90	12″ N of nucleus
1334a	110	0	4.5″ E of nucleus
1334b	5	0	through nucleus
1335	20	0	4.5″ E of nucleus
1339b	15	90	3″ N of nucleus

[a] All spectra taken at 54 Å mm^{-1} in the range 6300–6800 Å, except spectrum 1335 taken at 89 Å mm^{-1} in the range 3700–5100 Å.

took spectra of the nebulosity in 1976 with the 2.1 m telescope at McDonald Observatory. Then, in 1977, we obtained higher quality spectra with the 4 m telescope at Kitt Peak National Observatory, and these spectra are the sources of the spectrographic data presented here. The slit width was 1.3″. The dispersion on the spectra taken in the red is 54 Å mm^{-1} and is 89 Å mm^{-1} on the spectrum taken in the blue. The scale perpendicular to the dispersion is 25″ mm^{-1}. Data relative to the KPNO spectra are listed in Table 1. The slit positions are shown on Figure 1. Only one spectrum was taken in a position directly across the nucleus.

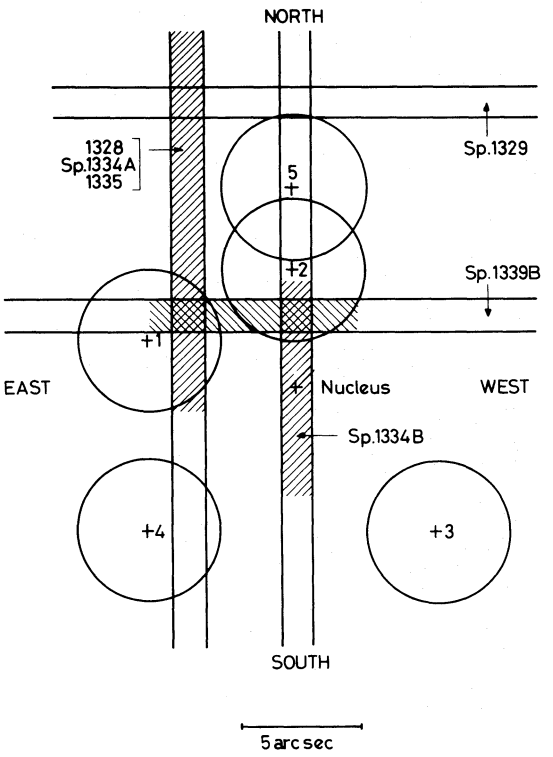

FIG. 1.—Positions of the spectrograph slit and of the IDS entrance aperture. Hatched areas along slit positions indicate detection of emission lines.

The lines of Hα, [N II] λλ6548, 6584, [S II] λλ6716, 6731, and several night-sky lines are seen on the spectra taken in the red. In the blue, the lines seen are [O III] λλ5007, 4959, Hβ, Hγ, Hδ, Hε + [Ne III] λ3967, [Ne III] λ3869, [O III] λ4363, and [O II] λ3727, and several absorption lines of the stellar population. A very weak line is present at the redshifted position of He II λ4686; its reality is confirmed by the spectrophotometric observations.

Examples of spectra are shown in Figures 2 and 3 (Plates 3 and 4). The intense continuum in the middle of each spectrum is emitted by the stellar population close to the center of the galaxy. The contrast between the intense stellar continuum and the rest of the spectrum reflects the rapid gradient of the surface brightness distribution of the stellar population near the center.

The emission lines show prominent condensations and weak extensions, which we refer to collectively as the nebulosity of ionized gas. On spectrum 1334a, the Hα line extends up to 30″ or 7.5 kpc NE of the nucleus. The brightest condensations seen on the spectra are located N to NW of the nucleus at distances ranging from 4″ to 8″. We found other bright clouds SW of the nucleus when we observed NGC 3516 with the IDS at KPNO (see § II*b*). There are also two small bright clouds 2″ N and 2″ S of the nucleus which could be considered as part of the central narrow-line region (Fig. 3, *top*). It is evident from the spectroscopic observations that the gas is unevenly distributed and extends over several kpc; this is confirmed by the IDS observations. It is interesting to note that on spectrum 1335 taken in the blue, no enhancement of the stellar continuum is detectable at the location of the bright condensation (Fig. 2, *bottom*).

The spectra were measured with the Interactive Picture Processing System at KPNO (Wells 1975) following the procedure outlined in Ulrich (1978). The two lines [N II] λλ6548, 6584 are contaminated by night-sky lines and were not measured except where very strong. The accuracy of the measurements, evaluated by comparing the measurements made on 1328 and 1334a, which were taken at the same position, is ±20 km s^{-1}. The accuracy is only ±40 km s^{-1} when estimated by comparing measurements made at the points where spectrum 1339b crosses spectra 1334a, 1334b, and 1335; this lower accuracy is due to the combined effects of the rapid velocity gradient and a slight uncertainty in tying together the angular distances on spectra taken in different positions. The lines are narrow with a width corresponding to no more than 250 km s^{-1}. The velocities of the gas with respect to the Sun are shown in Figure 4.

The velocity of the stars is known with a lower accuracy than that of the gas. We have only three measurements of absorption lines of stellar origin. The best one is from spectrum 1335, which gives $V_\odot$(stars) = 2650 km s^{-1} ± 70 km s^{-1}. The two other measurements are from IDS scans and give 2620 km s^{-1} at position 3 and 2570 km s^{-1} at position 4, with an error

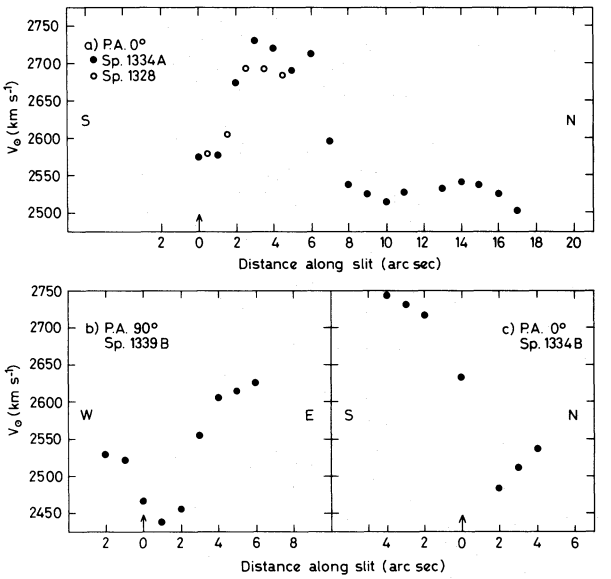

FIG. 4.—Velocity curves along three directions; arrows show points on slit which are closest to nucleus. Systemic velocity measured from stellar lines is 2650 ± 70 km s^{-1}. For details see text, § II*a*.

of ±150 km s^{-1}. We adopt $V_\odot = 2650$ km s^{-1} for the systemic velocity; this is in agreement with previous measurements (de Vaucouleurs, de Vaucouleurs, and Corwin 1976). After corrections for galactic rotation and taking the Hubble constant $H = 50$ km s^{-1} Mpc^{-1} the distance is 52 Mpc. At this distance 1″ corresponds to 250 pc.

The gas shows irregular motions. At the locations where we detected emission lines on the spectra, i.e., N and NW of the nucleus, the gas is approaching us at velocities up to 200 km s^{-1} with respect to the systemic velocity. Our spectrographic coverage being incomplete, we do not have accurate velocities SW of the nucleus.

The irregular motions observed cannot be explained by normal rotation motions of the galaxy. We attribute them to the presence of the Seyfert nucleus. Either the nucleus, during an explosion, has expelled the ionized gas now seen at several kpc from the nucleus, or this gas is ambient gas which was formerly neutral and which has been ionized and accelerated by radiation pressure from the ultraviolet (UV) continuum radiation of the Seyfert nucleus.

b) Spectrophotometric Observations

The nebulosity was observed with the two-channel IDS attached to the 2.1 m telescope at KPNO. The two entrance apertures of the IDS were 6″ in diameter and were separated by 90″. The wavelength resolution was 9 Å. First, a 5 minute integration was made at five locations around the nucleus (see Fig. 1). Then, 40 minute integrations were made in the red at location 3 and in the blue at locations 3 and 4. At location 4, the spectrum is purely stellar. The absence in the scans taken in positions 1–5 of any sign of a broad component of the hydrogen lines indicates that there is no contamination from the light emitted by the nucleus. Moreover, the [S II] line intensity ratio $I(6716)/I(6731)$ is definitely larger than one at locations 1, 2, 3, and 5, whereas Boksenberg and Netzer (1977) found it very close to one in the central narrow-line region. Two standard stars were also observed in order to transform the observed fluxes into absolute intensities (Oke and Schild 1970).

The equivalent width and absolute intensity of the Hα + [N II] λλ6548, 6583 line at different locations is given in Table 2. It is clear from this table that the gas is unevenly distributed around the nucleus. There is no appreciable difference between the line intensity ratios Hα/[N II] λ6584 and [S II] λ6717/[S II] λ6731 measured at locations 1, 2, 3, and 5; in the following it is assumed that the gas observed at location 3 is typical of the bright clouds in the nebulosity.

The observed line intensities at location 3 are given in Table 3. The scans in the blue at locations 3 and 4 and the scan in the red at location 3 are shown in Figures 5a and 5b.

The intensity of the continuum at location 4 is 85% of that measured at location 3. This is attributed to the fact that location 4 is closer to the minor axis of the inner region of the galaxy than location 3 and, therefore, is at a place where the surface brightness is less than at location 3. The intensities of the emission

TABLE 2

INTENSITIES OF Hα + [N II] λ6548, 6584 AT DIFFERENT LOCATIONS IN THE GASEOUS NEBULOSITY

Location Number	Distance from Center (arcsec)	Position Angle (degrees)	Equivalent Width of Hα + [N II] (Å)	Intensity of Continuum at 6500 Å × 10^{15} (ergs s^{-1} Å^{-1} cm^{-2})	I(Hα + [N II]) × 10^{14} (ergs s^{-1} cm^{-2})
1	6	70	3	1.1	0.3
2	5	0	57	3	17
3	8.5	225	62	0.85	5.3
4	8.5	135	0	0.72	0
5	8.5	0	15	1.1	1.7
Total (not including location 5)					= 22.6

TABLE 3

OBSERVED LINE INTENSITIES IN THE NEBULOSITY AT LOCATION 3

Emission Line	Ion	Line Intensities × 10^{16} (ergs cm^{-2} s^{-1})	$I/I(H\beta)$
3727	O II	153	2.55
3869	Ne III	47	0.80
4340	H	26	0.43
4363	O III	7	0.12
4686	He II	19	0.30
4861	H	60	1
4959	O III	193	3.2
5007	O III	601	10
6300	O I	27	0.45
6548	N II	80	1.3
6563	H	212	3.5
6584	N II	239	4
6717	S II	97	1.4
6731	S II	50.8	0.90

lines, in particular He II λ4686, [O III] λ4363, and Hγ were measured on the spectrum obtained by subtracting 1.17 times the scan at location 4 from the scan at location 3. The errors on the measurements of the line intensities are $\pm 50\%$ on the four weakest lines and $\pm 30\%$ on the other lines.

The line intensities corrected for reddening (see § III*a*) with $c = 0.34$ and $c = 0.71$ are given in Table 4, columns (3) and (4). In the following, we base our discussion of theoretical models on the intensities dereddened with $c = 0.34$. Choosing instead the dereddened intensities obtained with $c = 0.71$ would not change our conclusions. Column (6) of Table 4 gives the line intensities of an average Seyfert type 2 galaxy or narrow-line radio galaxy (Koski 1978, Table 9).

Table 3 gives several interesting indications of the state of the gas in the gas clouds. The ratio [S II] λ6717/[S II] λ6731 indicates $N_e < 400$ cm^{-3}, i.e., definitely less than in the narrow-line region of the Seyfert nucleus (Boksenberg and Netzer 1977). At low densities, the ratio of the [O III] lines $I(5007)/I(4363)$ is a temperature indicator which in the present case gives $T_e \lesssim 15{,}000$ K. This rules out an excitation by shock waves (Cox 1972; Dopita 1977). Table 3 also shows that the spectrum of the extended nebulosity in NGC 3516 has striking similarities with the spectrum of Seyfert type 2 nuclei, except that in general the latter have larger electron densities (e.g., Koski 1978). These qualitative characteristics of the gas, as well as the fact that there is no sign of a young stellar population at the location of the gas clouds (spectrum 1335, Fig. 2, *bottom*), has led us to explore photoionization models of the nebulosity where the ionizing radiation is the nonthermal radiation emitted by the nucleus. These models are presented in the next section.

III. PHOTOIONIZATION MODELS

a) Input Parameters

In these models, a central source of ionizing radiation of absolute luminosity L_ν illuminates a nebulosity at a distance R. The ionizing flux incident on the nebulosity is $\phi = L_\nu(4\pi R^2 h\nu)^{-1}$ photons cm^{-2} s^{-1} ryd^{-1}. In the part of the nebulosity located at location

TABLE 4

OBSERVED EMISSION LINE INTENSITIES CORRECTED FOR REDDENING AND CALCULATED INTENSITIES

Emission Line (1)	Ion (2)	Observed $I/I(H\beta)$ $c = 0.34$[a] (3)	Observed $I/I(H\beta)$ $c = 0.71$ (4)	Calculated $I/I(H\beta)$ Model M1[b] (5)	Typical Seyfert Type 2 or NLRG[c] (6)
1548 + 1551	C IV	...	...	3.3	...
1907 + 1909	C III	...	...	8.0	...
2795 + 2803	Mg II	...	...	1.9	...
3346 + 3426	Ne V	...	...	1.3	1.4
3726 + 3729	O II	3.2	4.1	3.7	3
3869 + 3968	Ne III	1.2	1.5	1.0	1.9
4363	O III	0.16	0.20	0.16	0.2
4686	He II	0.33	0.37	0.30	0.3
4861	H	1	1	1	1
4959 + 5007	O III	12.9	12.5	12.4	15
5198 + 5200	N I	...	...	0.1	...
5876	He I	...	...	0.10	0.1
6300 + 6363	O I	0.47	0.37	0.42	0.5
6312	S III	...	...	0.07	...
6563	H	2.7	2.1	2.8	2.7
6548 + 6584	N II	4.1	3.1	3.5	3.1
6717 + 6731	S II	1.9	1.4	0.84	1.5
9069 + 9532	S III	...	...	2.1	...

[a] $I(H\beta) = 1.3 \times 10^{-14}$ ergs cm^{-2} s^{-1}.

[b] Model with $n_H = 30$, $\tau_{13.6} = 1400$, and [O] $= 3 \times 10^{-4}$.

[c] Adapted from Koski 1978 (Table 9). Intensities of Ne V, Ne III, O III, and N II include both components of each doublet.

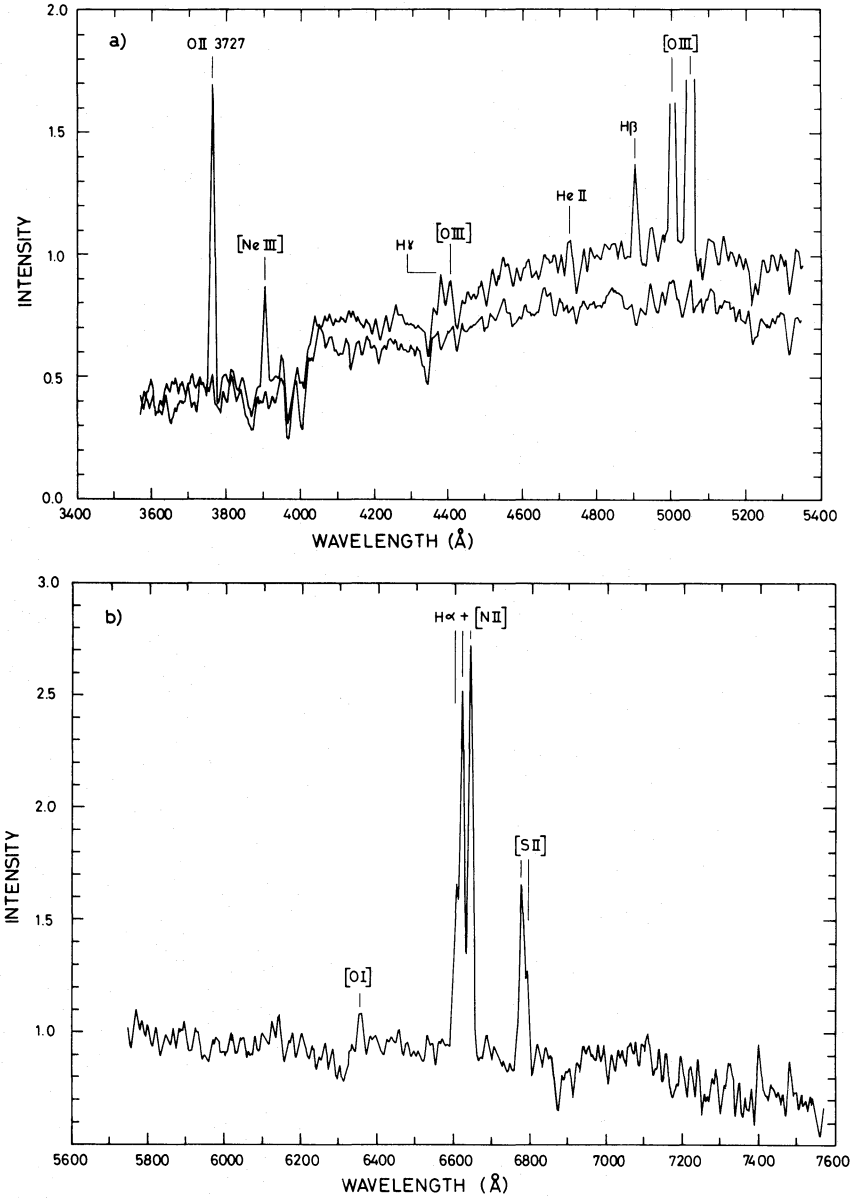

FIG. 5.—IDS scans of nebulosity of NGC 3516 with entrance aperture located at 8.5″ or 2 kpc from nucleus. *Top:* positions 3 and 4, blue wavelength range. *Bottom:* position 3, red wavelength range.

3, i.e., at 8″ from the nucleus, R is $=10^7$ cm. The luminosity of the continuum source in the nucleus of NGC 3516 derived from observations done with the *International Ultraviolet Explorer* satellite is $L'_\nu \approx 10^{27}$ ergs s^{-1} Hz^{-1} at 1300 Å (Ulrich, in preparation). The reddening correction to be applied to L'_ν to obtain L_ν is uncertain and depends on the amount of intervening material on the path of light from the central continuum source to Earth and to the nebulosity. At $\lambda = 1300$ Å, the correction to be applied to L'_ν is $10^{2.48c}$, where c is the normal reddening coefficient (Nandy *et al.* 1975). The minimum value of c is ~ 0.16, which is the reddening in our Galaxy at $b = 42°$, the galactic latitude of NGC 3516. The value of c derived from $I(\mathrm{H}\alpha)/I(\mathrm{H}\beta)$ in the narrow-line region in the nucleus is 0.71. Finally, the ratio $I(\mathrm{H}\alpha)/I(\mathrm{H}\beta)$ in the extended nebulosity studied here corresponds to $c = 0.34$. The calculations were performed with $L_\nu = 10^{28}$ ergs s^{-1} Hz^{-1}, which corresponds to $c = 0.4$, and a power-law spectrum of the form $f_\nu \propto \nu^{-1}$. This value of L_ν corresponds to $\phi = 1.7 \times 10^9$ photons cm^{-2} s^{-1} ryd^{-1} at $h\nu = 1$ rydberg.

The results of the model calculations depend primarily on ϕ/n_{H} (MacAlpine 1976). Thus, the calculated line ratios do not change if $L_\nu R^{-2}$ and n_{H} are multiplied by the same factor. The line intensities are proportional to $\Omega/4\Pi$, where Ω is the solid angle covered by the nebulosity viewed from the central

source; and, therefore, for a given set of observed line intensities, $\Omega/4\Pi$ is proportional to L_ν^{-1}.

Unless otherwise stated, the calculations were performed with roughly normal abundances, namely: [He] = 0.1, [C] = 3×10^{-4}, [N] = 1×10^{-4}, [O] = 6×10^{-4}, [Ne] = 1×10^{-4}, [Mg] = 3×10^{-5}, and [S] = 1.5×10^{-5} (by numbers relative to H).

b) Calculations

The program used in the calculations is a standard program to obtain the ionization and temperature equilibrium at each point of the gas (e.g., Aldrovandi and Stasińska 1978). The photoionization of atomic inner shells, the Auger effect, and the secondary ionizations of H and He by photoelectrons are fully considered. The transfer of the ionizing diffuse field is treated in the "outward only" approximation, along 20 directions, under the assumption of spherical symmetry or $\Omega/4\Pi = 1$, i.e., the nebulosity as seen from the central ionizing source covers a 4Π solid angle. The transfer of the resonant lines and the Bowen fluorescence are treated in a "straight-line path" approximation. All the discontinuities of the primary and diffuse continua are taken into account. In a typical run, the nebula is divided into 100 concentric layers. The atomic parameters used include the collision strengths of [S II] and of [Ne V] recently published by Pradhan (1978) and by Giles (1979), respectively.

It is well known that photoionization models give line intensities which are too low for the low and intermediate excitation lines; this is true not only in nuclei of galaxies (NGC 3516 is a typical example; see Boksenberg and Netzer 1977), but also in galactic nebulae where there is little doubt that photoionization is the cause of excitation. A detailed study of the planetary nebula NGC 7027, which has a spectrum which is particularly rich and accurately observed, led Péquignot, Aldrovandi, and Stasińska (1978) and Péquignot, Stasińska, and Aldrovandi (1979) to introduce empirically charge-transfer reactions between atomic hydrogen and a number of ions (O^{+2}, S^{+3}, Ne^{+2}, N^{+2}) in order to eliminate the discrepancies which systematically appear between the observations and the calculations made with simple, but realistic, models. Taking a different approach, Dalgarno and Butler (1978) have shown from theoretical considerations, that charge-transfer reactions of N^{+2} and S^{+3} should be fast. Very recently, Butler, Bender, and Dalgarno (1979) have calculated the charge-transfer rate coefficient for O^{+2} and found a value in agreement with that deduced from models by Péquignot, Stasińska, and Aldrovandi (1979).

The rate coefficients for charge-transfer reactions used in our calculations are listed in Table 5. Since $\beta(Ne^{++})$ is uncertain,[3] we have also made calculations with $\beta(Ne^{++}) = 0$; the line intensities are not affected by the value of $\beta(Ne^{++})$, except that the intensities of the [Ne III] lines are larger by a factor 1.4 for $\beta(Ne^{++}) = 0$.

TABLE 5

CHARGE-TRANSFER RATE COEFFICIENTS WITH H^0 (in $cm^3\ s^{-1}$)

Ion	Rate[a]	Reference
He^+	1.9×10^{-15}	1
He^{++}	1.56×10^{-13}	2
C^{+3}	1.6×10^{-9}	3
C^{+4}	1.0×10^{-9}	4
N^+	2.2×10^{-12}	5, 6[b]
N^{+2}	$10^{-9} \times T_4$	6
N^{+3}	$3 \times 10^{-9} \times T_4$	7
O^+	10^{-9}	8[b]
O^{+2}	8×10^{-10}	6
Ne^{+2}	2×10^{-10}	6
S^{+3}	$1.5 \times 10^{-9} \times T_4$	6

[a] T_4 is $10^{-4}T$.

[b] Inverse reaction with H^+ included.

REFERENCES.—(1) Jura and Dalgarno 1971. (2) Arthurs and Hyslop 1957. (3) Watson and Christensen 1979. (4) Valiron 1978. (5) Melius 1973. (6) Péquignot, Aldrovandi, and Stasińska 1978, and Péquignot, Stasińska, and Aldrovandi 1979. (7) Christensen, Watson, and Blint 1977. (8) Field and Steigman 1971.

c) Results

The results[4] are presented as curves giving the line intensities relative to Hβ as a function of n_H, in the optically thin case, $\tau_{13.6} < 3$ (Fig. 6*a*), and in the radiation bounded case, i.e., with $\tau \approx \infty$ (Fig. 6*b*). (The radiation bounded case is defined here by the condition that the gas temperature falls below 3000 K.) The observed de-reddened fluxes (column [3] of Table 4) are represented by dots on the appropriate curves.

Examination of Figures 6*a* and 6*b* leads to the following conclusions:

i) The observed intensity of [O I] λ6300 can be reproduced in an optically thin model only if $n_H > 500\ cm^{-3}$; this is not compatible with the ratio of the S II lines $I(6731)/I(6717)$, and therefore an optically thin model is not adequate. Moreover, in an optically thin model the physical thickness of the emitting region would be extremely small, of the order of 5×10^{16} cm, compared to the other dimensions of the clouds or filaments; this geometry appears very unlikely. For these reasons, we will not consider the optically thin models any further in this section.

ii) The optically thick model can reproduce rather well the relative line intensities of O I, O II, and O III for a density n_H between 10 and $100\ cm^{-3}$, and it is concluded that it is appropriate to the nebulosity of NGC 3516.

[3] $\beta(X^m)$, in units of $cm^3\ s^{-1}$, corresponds to the reaction: $H + X^m \rightarrow H^+ + X^{m-1}$.

[4] This model is appropriate to any nebulosity of moderate density exposed to an ionizing radiation with a power-law spectrum; we give the calculated intensities not only for the lines observed in the nebulosity of NGC 3516 but also for UV and weak optical lines.

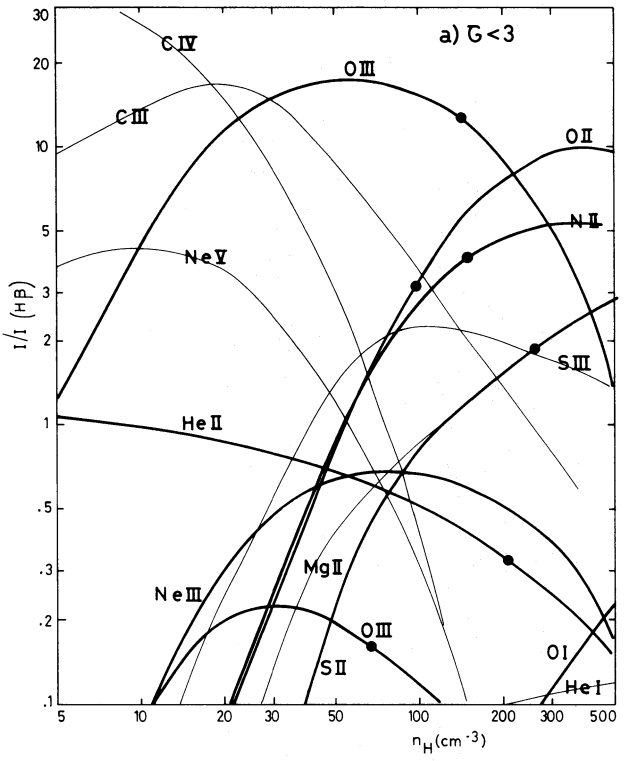

FIG. 6a

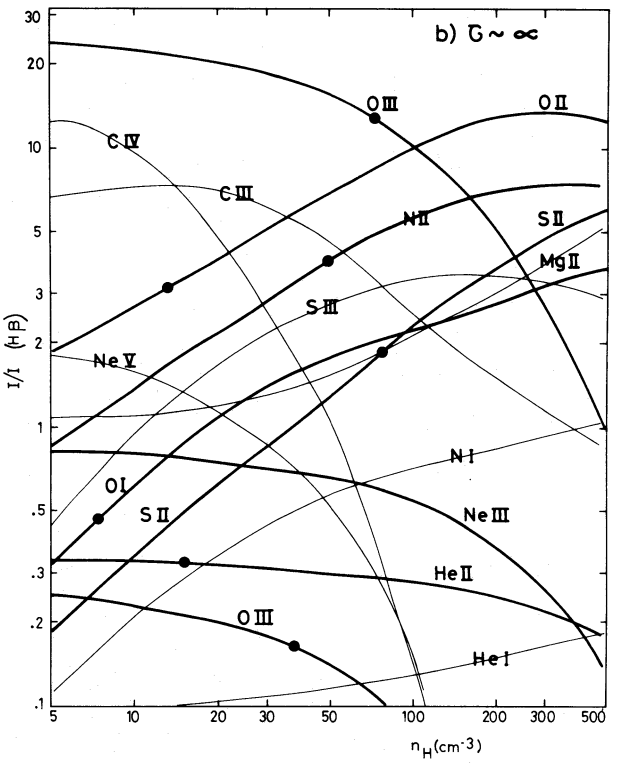

FIG. 6b

FIG. 6.—Line intensities relative to Hβ for photoionization models which include the charge-transfer reactions of Table 5. The incident radiation has a ν^{-1} spectrum with $\phi = 1.7 \times 10^9$ photons cm^{-2} s^{-1} ryd^{-1} at $h\nu = 1$ ryd. (*a*) Optically thin case $\tau_{13.6} < 3$. (*b*) Radiation bounded case which is equivalent to $\tau_{13.6} = \infty$. The line wavelengths are given in column (1) of Table 4; on each graph, 2 curves are labeled O III: the top one corresponds to [O III] λ5007 + 4959 and the bottom one to [O III] λ4363. The dots indicate observed intensities corrected for reddening with $c = 0.34$ from column (3) of Table 4. (The observed intensity of [Ne III] does not correspond to any point on the Ne III curve with the set of elemental abundances adopted in the calculations.)

The calculations are valid for any nebulosity where the collisional de-excitation can be neglected ($n_H < 10^3$ cm^{-3}); the intensity of some UV lines and weak optical lines are given together with the lines observed in the nebulosity of NGC 3516.

The intensity of [O III] λ5007, the most accurately observed of the oxygen lines, relative to Hβ, is a little too large for the value of the oxygen abundance, [O] $= 6 \times 10^{-4}$, with which the model was calculated. We computed another model with [O] $= 3 \times 10^{-4}$, [C] $= 2 \times 10^{-4}$, and the other abundances given in § III*a*, and with $\tau_{13.6} = 1400$ and $n_H = 30$ cm^{-3}. The line intensities in this model, called model M1, are listed in Table 4, column (5). These are in very good agreement with the observed, de-reddened line intensities in columns (3) and (4). In model M1, the geometrical thickness of the emitting region is $\Delta R = 1.8 \times 10^{19}$ cm. Hydrogen is neutral in a large fraction of the emitting region, and this is where most of the emission from the O I and S II lines occurs. We have also computed a model which is essentially radiation bounded with $\tau_{13.6} = 8500$. One expects that this model would differ from M1 essentially only by the strength of the lines of O I and S II. This completely thick model gives

$$I([\text{O I}]\ \lambda 6300, 6363)/(\text{H}\beta) = 0.75$$

and

$$I([\text{S II}]\ \lambda 6717, 6731)/(\text{H}\beta) = 1.07\,,$$

which is fairly close to the values given by M1 and not incompatible with the observations. It follows that model M1 is valid for any value of ΔR larger than a few parsecs.

Test calculations show that the value $\tau_{13.6}$, and therefore the derived mass of the emitting gas (see below), depends moderately on the choice of the incident spectrum in the far-UV and soft X-ray range. We have just seen that, with a spectrum $f_\nu \propto \nu^{-1}$, [O I] λ6300 is compatible with a completely optically thick case—or radiation bounded case; this rules out a steeper ionizing spectrum, because with such a steep spectrum [O I] would be weaker than observed. On the other hand, if, as suggested by the emission line spectrum of the nucleus, and in particular by the large intensities of [O I] λ6300 and [Ne V] λ3426 (Boksenberg and Netzer 1977), the primary spectrum is somewhat harder than ν^{-1}, then the nebulosity outside the nucleus could consist of filaments of

various optical thicknesses, some being radiation bounded. Information on the intensity of [Ne V] λ3426 in the nebulosity would help in restricting these possibilities.

Finally, we note that model M1 gives I(S II λ6717, 6731)/Hβ too small by a factor of 2. No useful comment can be made on this point, however, in the absence of information on the other ionization stages of sulfur.

d) Mass of the Emitting Gas

In the optically thick models, the Hβ intensity calculated with the assumption of spherical symmetry, i.e., $\Omega/4\Pi = 1$, and with $L_\nu = 10^{28}$ ergs s^{-1} Hz^{-1} is $I(\mathrm{H}\beta) = 1.5 \times 10^{-12}$ ergs cm^{-2} s^{-1}. The observed de-reddened Hβ intensity at location 3 is 1.3×10^{-14} ergs s^{-1} cm^{-2}; therefore, the solid angle Ω covered by the clouds at location 3 is $\Omega/4\Pi \approx 10^{-2}$. The mass of emitting gas at location 3, calculated with model M1, with $n_{\mathrm{H}} = 30$ and $\tau_{13.6} = 1400$, is

$$M = (\Omega/4\Pi)4 \times 10^8\ M_\odot = 4 \times 10^6\ M_\odot\ .$$

We emphasize that the derived mass depends only on ϕ/n_{H}, which is determined to better than a factor of 2 by the ratio of the O II and O III lines, and on $\tau_{13.6}$, which is determined by the intensity of [O I] λ6300. Note that most of this mass resides in the large fraction of the emitting region where H is essentially neutral.

Table 2 shows that the whole nebulosity emits $I(\mathrm{H}\alpha) = 22.6 \times 10^{-14}$ ergs cm^{-2} s^{-1} or $\sim$4 times more than location 3. It follows that, with the assumption that the gas at location 3 is typical of the whole nebulosity detected with the IDS, the total mass of the emitting gas is $1.6 \times 10^7\ M_\odot$.

The lower limit of the mass of neutral hydrogen detectable in the 21 cm line is therefore $\sim 10^7\ M_\odot$. For comparison, the most recent 21 cm observation of NGC 3516 gives an upper limit to the mass of neutral hydrogen of $10^9\ M_\odot$ (Heckman, Balick, and Sullivan 1978).

IV. DISCUSSION AND CONCLUSIONS

a) Physical Conditions of the Gas at Location 4, Where No Emission Lines are Detected

It is worth investigating whether any useful information on the state of the gas can be obtained from the fact that no lines are detected at location 4, which is at the same distance from the ionizing source as location 3 where a rich emission line spectrum is observed.

The absence of detected emission at location 4 may be explained in two ways:

1. No significant amount of ionizing radiation reaches location 4, and the gas, if present, is neutral and cold. This implies that the material in the nucleus is opaque to the ionizing radiation in the direction of location 4. We see ionized gas *only* in the directions along which the radiation can escape from the nuclear region; specifically, the radiation escapes in two opposite directions: N to NE and SW of the nucleus.

2. Alternatively the radiation escaping from the nucleus is isotropic on a large scale, and as much radiation reaches location 4 as location 3. The gas can still be undetectable at location 4 in the following circumstances:

i) The gas is optically thick to ionizing radiation and is clumped in small, very dense clouds, which together cover a very small solid angle. Figure 6*b* shows that the most prominent lines in the spectrum of these dense optically thick clouds should be the low-excitation lines [O II], [N II], and [S II]. The nondetection of [O II] λ3727 in location 4 [which means I(O II) at location 4 is less than $\sim 0.3I(\mathrm{H}\beta)$ at location 3, i.e., less than 2×10^{-15} ergs cm^{-2} s^{-1}] implies that the solid angle covered by these small dense clouds is less than 0.1 times the solid angle covered by the gas at location 3.

ii) The gas is optically thin. Figure 6*a* shows that for $n_{\mathrm{H}} < 5$ the nondetection of Hβ sets more stringent limits than the nondetection of [O III] λ5007. Calculations show that Hβ is undetectable if the mean optical thickness of the gas in the observed volume is less than ~ 1. The maximum mass of gas at location 4 which remains invisible is obtained with the assumption that the gas is uniformly distributed with a filling factor of one; in this case, and with $n_{\mathrm{H}} \lesssim 1$, $M_{\max}$ is $1.5 \times 10^6\ M_\odot$. For density larger than $n_{\mathrm{H}} = 1$, the mass of invisible ionized gas decreases as n_{H}^{-2} up to $n_{\mathrm{H}} = 5$ and decreases even more rapidly with increasing density for $n_{\mathrm{H}} > 5$, because the limits set by the nondetection of [O III] λ5007 are more stringent than for Hβ.

b) Concluding Remarks

The bright ionized clouds in the extended nebulosity in NGC 3516 have an emission line spectrum very similar to that of Seyfert type 2 galaxies and narrow line radio galaxies (Koski 1978, Table 9). The models where the clouds at 2 kpc from the center are ionized by the central continuum source with a power-law spectrum of $f_\nu \propto \nu^{-1}$ fit the observed line intensities well. The main difference between the physical conditions of the gas in the Seyfert type 2 galaxies and in the nebulosity of NGC 3516 is that in the latter the particle density is only ~ 30 cm^{-3} as compared with 500 cm^{-3} or more in the former.

Shock-wave models cannot account for the presence of He II λ4686 and for the relative strengths of the oxygen lines ([O III] λ5007 and [O I] λ6300 should be weaker and stronger, respectively; see Dopita 1977). The abundances deduced from the models are close to what is usually found in galactic nebulae: this attests that the gas has been efficiently processed by nucleosynthesis.

The nebulosities associated with a number of radio galaxies and quasars, for example 3C 120 (Baldwin *et al.* 1980) and 3C 48 (Wampler *et al.* 1975), have a high-excitation spectrum and in that respect bear some

resemblance to the nebulosity of NGC 3516. However, in the cases of 3C 48 and 3C 120, the nebulosities extend to larger distances from a nucleus which itself is much brighter than the nucleus of NGC 3516. It is not clear whether the nebulosity of NGC 3516 is a scaled-down version of the nebulosities seen in these more distant objects. A common problem associated with all these nebulosities is that their origin is unknown. So far the data are compatible with the following possible origins: (1) the nebulosity has been ejected from the nucleus, (2) the nebulosity is formed by formerly neutral ambient gas excited and accelerated by the Seyfert or quasar nucleus, or (3) the nebulosity is formed by ambient gas which is now falling on the nucleus and which starts radiating effectively in the optical range when it reaches the appropriate density and distance from the center. Note that in this last case, the gas is not primeval, since the elemental abundances are nearly normal in the nebulosity.

The support of the National Science Foundation, through grant AST 73-05312, during part of this work, is gratefully acknowledged.

REFERENCES

Adams, T. F. 1977, *Ap. J. Suppl.*, **33**, 19.
Aldrovandi, S. M. V., and Stasińska, G. 1978, *Rev. Brasileira Fis.*, **8**, 595.
Andrillat, Y., and Souffrin, S. 1973, *Ap. Letters*, **1**, 11.
Arthurs, A. M., and Hyslop, J. 1957, *Proc. Phys. Soc. London*, A **70**, 849.
Baldwin, J. A., Carswell, R. R., Wampler, J. E., Smith, H. E., Burbidge, E. M., and Boksenberg, A. 1980, **236**, 000.
Boksenberg, A., and Netzer, H. 1977, *Ap. J.*, **212**, 37.
Butler, S. E., Bender, C. F., and Dalgarno, A. 1979, *Ap. J. (Letters)*, **230**, L59.
Christensen, R. B., Watson, W. D., and Blint, R. J. 1977, *Ap. J.*, **213**, 712.
Cox, D. P. 1972, *Ap. J.*, **178**, 143.
Dalgarno, A., and Butler, S. E. 1978, *Comments At. Mol. Phys.*, **7**, 129.
de Vaucouleurs, G., and de Vaucouleurs, A. 1972, *Ap. Letters*, **12**, 1.
de Vaucouleurs, G., de Vaucouleurs, A., and Corwin, H. G. 1976, *Second Reference Catalogue of Bright Galaxies* (Austin: University of Texas Press).
Dopita, M. A. 1977, *Ap. J. Suppl.*, **33**, 437.
Field, G. B., and Steigman, G. 1971, *Ap. J.*, **166**, 59.
Giles, D. 1979, *M.N.R.A.S.*, **187**, 49P.
Heckman, T. M., Balick, B., and Sullivan, W. T. 1978, *Ap. J.*, **224**, 745.
Jura, M., and Dalgarno, A. 1971, *Astr. Ap.*, **14**, 243.
Koski, A. T. 1978, *Ap. J.*, **223**, 56.
MacAlpine, G. M. 1976, *Ap. J.*, **204**, 694.
Melius, C. F. 1973, in *Abstracts of Papers VIII ICPEAC* (Belgrade), ed. B. C. Čobić and M. V. Kupera.
Nandy, K., Thompson, G. I., Jamar, C., Monfils, A., and Wilson, R. 1975, *Astr. Ap.*, **44**, 195.
Oke, J. B., and Schild, R. E. 1970, *Ap. J.*, **161**, 1015.
Péquignot, D., Aldrovandi, S. M. V., and Stasińska, G. 1978, *Astr. Ap.*, **63**, 313.
Péquignot, D., Stasińska, G., and Aldrovandi, S. M. 1979, *Astr. Ap.*, in press.
Pradhan, A. K. 1978, *M.N.R.A.S.*, **183**, 89P.
Ulrich, M.-H. 1978, *Ap. J.*, **219**, 424.
Valiron, P. 1978, private communication.
Wampler, E. J., Robinson, L. B., Burbidge, E. M., and Baldwin, J. A. 1975, *Ap. J. (Letters)*, **198**, L49.
Watson, W. D., and Christensen, R. B. 1979, *Ap. J.*, **231**, 627.
Wells, D. 1975, *KPNO–CTIO Quart. Bull.*, July-September, p. 12.

Note added in proof.—NGC 3516 was reobserved in 1980 February. At location 3, the intensity of [Ne v] λ3426 is $\sim$1.2 times that of Hβ, in good agreement with the model M1.

D. Péquignot: Observatoire de Meudon, 92190 Meudon, France
Marie-Helene Ulrich: European Southern Observatory, CERN, 1211 Geneva 23, Switzerland

PLATE 3

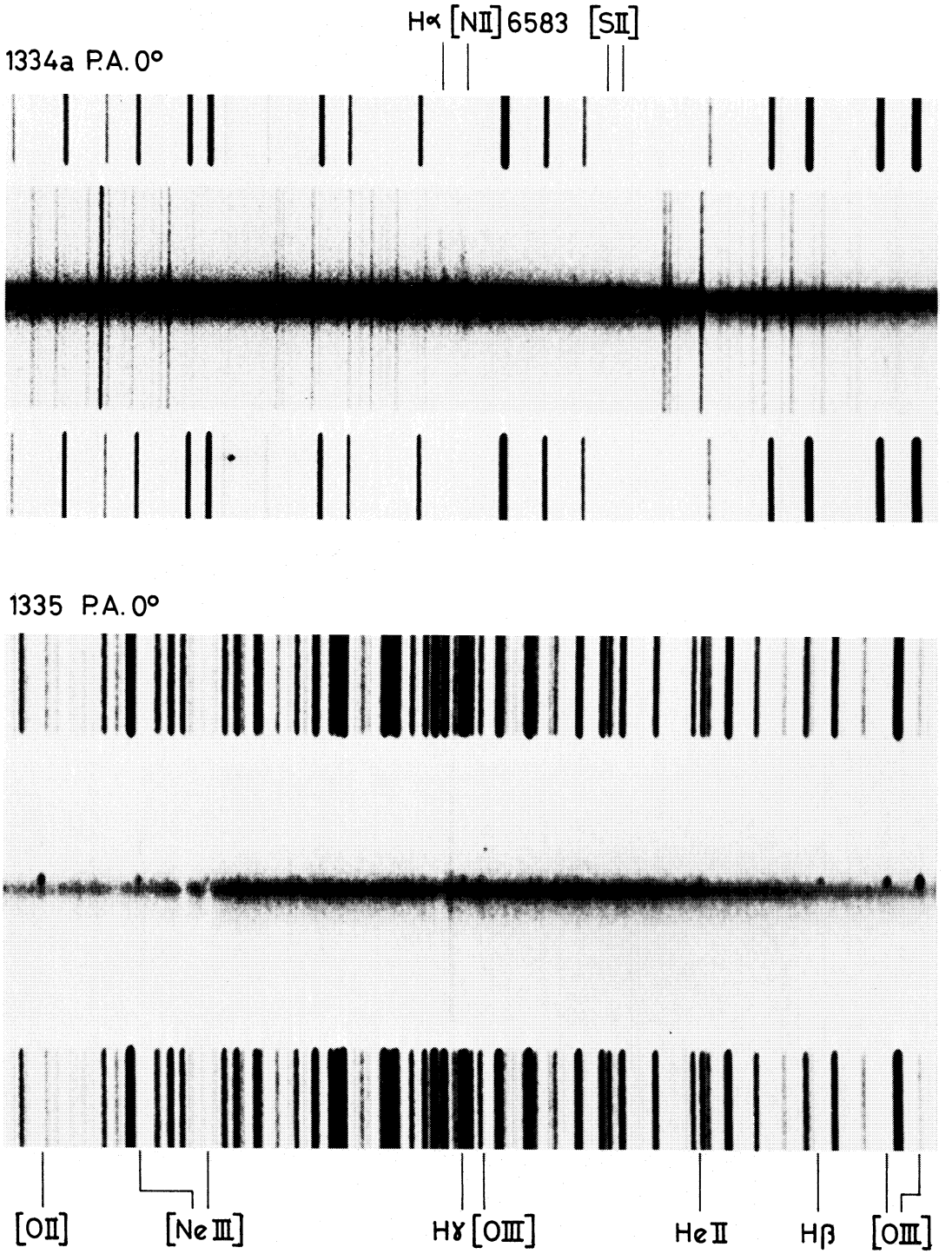

FIG. 2.—Spectrograms taken across the ionized nebulosity in NGC 3516. Spectra were taken with the 4 m telescope at KPNO. For both spectra slits were at 4.5″ E of nucleus and oriented in NS direction. Original scale perpendicular to the dispersion of 25″ mm^{-1}. *Top:* spectrum 1334a—original dispersion 54 Å mm^{-1}. Distance between inner edges of comparison spectrum is 125″. *Bottom:* spectrum 1335—original dispersion 89 Å mm^{-1}. Distance between inner edges of comparison spectrum is 143″.

ULRICH AND PÉQUIGNOT (*see* page 46)

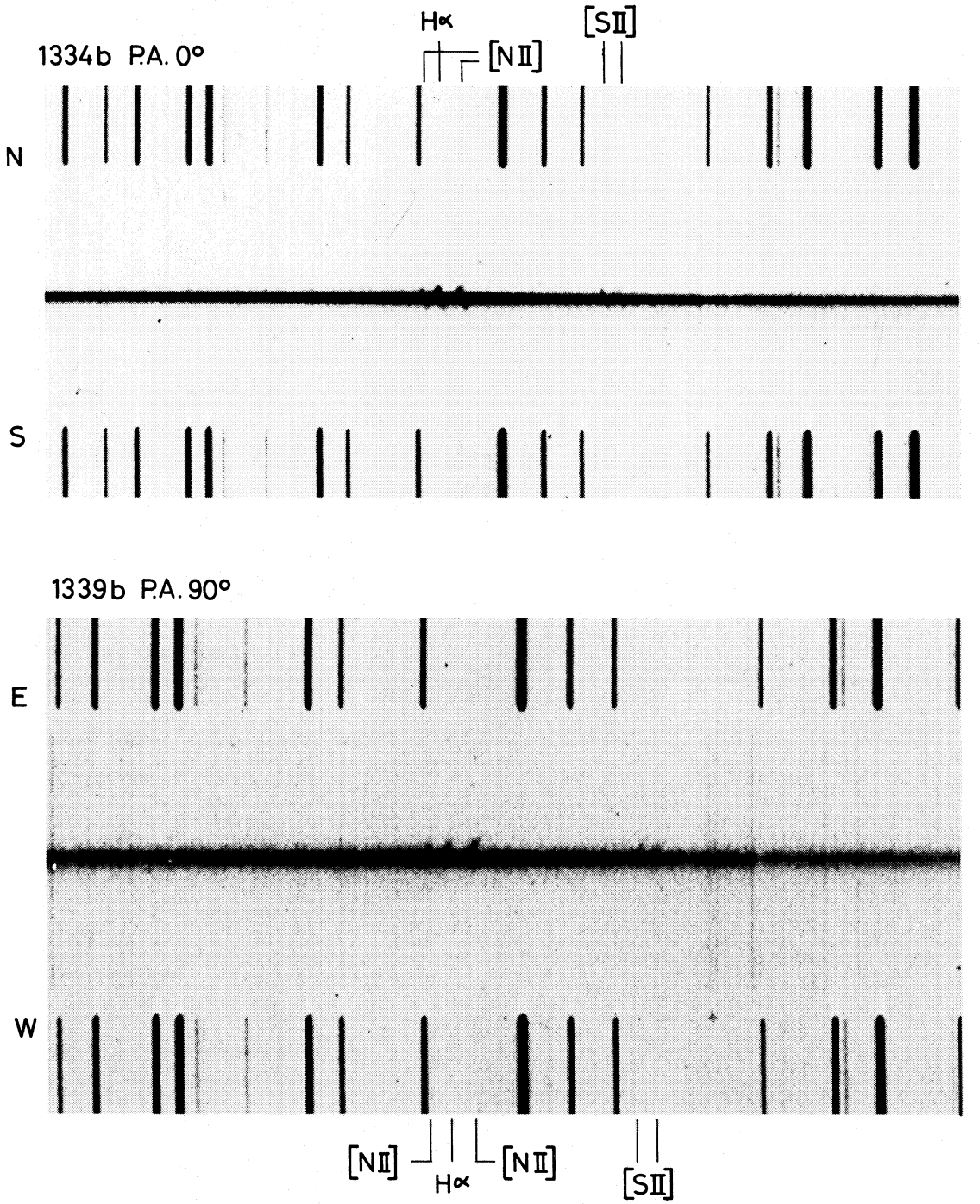

FIG. 3.—Spectrograms taken across the ionized nebulosity in NGC 3516. Spectra were taken with the 4 m telescope at KPNO. Original dispersion 54 Å mm^{-1}. Distance between inner edges of comparison spectrum is 125″. *Top:* spectrum 1334b—5 minute exposure spectrum through nucleus; clouds N and S of nucleus are a part of the narrow-line region in the nucleus. *Bottom:* spectrum 1339b—taken with slit 3″ N of nucleus in EW direction.

ULRICH AND PÉQUIGNOT (*see* page 46)